

# MEOH TO DME IN BUBBLING FLUIDIZED BED: EXPERIMENTAL AND MODELLING

Mads Kaarsholm,<sup>1</sup>\* Finn Joensen,<sup>2</sup> Roberta Cenni,<sup>2</sup> Jamal Chaouki<sup>1</sup> and Gregory S. Patience<sup>1</sup>

1. Department of Chemical Engineering, École Polytechnique de Montréal, Montreal, Quebec, Canada

2. Haldor Topsøe A/S, Lyngby, Denmark

Methanol dehydration over a ZSM-5 containing catalyst was studied in a fluidized bed reactor. At temperatures ranging from 250 to 325°C, methanol conversion varied from 30% at a contact times of 0.14 s and approached 100% of the equilibrium conversion at a contact time starting from 10 s. Sequential and parallel reactions were negligible at low temperatures while hydrocarbon formation became appreciable at 325°C. Online gas analysis by mass spectrometry provided real-time measurements at a frequency of 4.4 Hz that allowed for fast determination of steady-state conditions. Gas phase residence time distribution (RTD) measurements indicated that axial dispersion was essentially negligible at short contact times with a shallow bed of catalyst. With longer residence times, the flow pattern could be approximated by six continuously stirred-tank reactors (CSTR) in series. Both the simple 1D hydrodynamic model and a detailed multi-zone fluidized model were used to interpret the experimental data to derive a kinetic expression for the dehydration of methanol to di-methyl ether (DME). The expression includes the reverse reaction that is most often neglected in the literature. The reaction data were best fit with the kinetics based on the 1D model. The fluidized bed is a viable reactor type for kinetic measurements of highly exothermic reactions where hotspots and radial and axial temperature gradients are problematic in fixed beds.

La déshydratation du méthanol sur un catalyseur contenant du ZSM-5 était étudiée dans un réacteur à lit fluidisé. À des températures allant de 250 à 325°C, la conversion du méthanol variait à partir de 30% à un temps de contact de 0,14 s et approchait de 100% de la conversion de l'équilibre à un temps de contact commençant à partir de 10 s. Les réactions séquentielles et parallèles étaient négligeables à des températures basses, alors que la formation d'hydrocarbure devenait appréciable à 325°C. Une analyse du gaz en ligne par spectroscopie de masse a fourni des mesures en temps réel à une fréquence de 4,4 Hz, ce qui permettait une détermination rapide de conditions d'état permanent. Les mesures de la distribution des temps de séjour (DTS) de la phase gazeuse ont indiqué que la dispersion axiale était essentiellement négligeable à des temps de contact courts avec un lit peu profond de catalyseur. Avec des temps de séjour plus longs, on pourrait approximer le modèle d'écoulement par six réacteurs à cuve agitée en continu en série. À la fois le modèle hydrodynamique 1-D simple et un modèle fluidisé multizones détaillé ont été utilisés pour interpréter les données expérimentales afin de trouver une expression cinétique pour la déshydratation du méthanol en méthoxyméthane. L'expression comprend la réaction inverse qui est très souvent négligée dans la littérature. Les données de réaction concordaient le mieux avec la cinétique fondée sur le modèle 1-D. Le lit fluidisé constitue un type de réacteur viable pour les mesures cinétiques de réactions très exothermiques pour lesquelles des points chauds ainsi que des gradients de température radiaux et axiaux constituent un problème pour les lits fixes.

**Keywords:** methanol dehydration, DME, fluidized bed, *n*-CSTR in series, reaction kinetics

## INTRODUCTION

The dehydration of methanol over an acidic catalyst is an important reaction for the production of di-methyl ether (DME). DME is considered as one of the best alternatives to diesel fuel with decreased NO<sub>x</sub>, CO, and hydrocarbon emissions with both lower particle emissions and lower global warming potential than conventional fuels (Gray and Webster,

\*Author to whom correspondence may be addressed.

E-mail address: [mkaa@topsoe.dk](mailto:mkaa@topsoe.dk)

Can. J. Chem. Eng. 89:274–283, 2011

© 2010 Canadian Society for Chemical Engineering

DOI 10.1002/cjce.20386

Published online 31 August 2010 in Wiley Online Library ([wileyonlinelibrary.com](http://wileyonlinelibrary.com)).

2001; Semelsberger et al., 2006). The reaction is also important as the first step to produce olefins (MTO) or gasoline (MTG) (Keil, 1999).

Several authors have investigated the dehydration reaction over different catalysts including alumina, silica-alumina, or acidic iron exchange resins. Most kinetic expressions are based on either the Langmuir–Hinshelwood or the Eley–Rideal mechanisms and account for the adsorption of water and methanol but neglect the contribution of DME since its absorption constant is considered insignificant. Berčić and Levec (1992); and Mollavali et al. (2008) have summarised many of the models presented in the literature and have also studied the intrinsic reaction kinetics. Most of the kinetic expressions have assumed that the reaction was irreversible, thus neglecting the reduction in reaction rate as the gas composition approaches equilibrium, which is critical for industrial applications.

Often reaction rate kinetics are measured in fixed beds under differential conditions. The main advantage of the fixed bed is that the flow pattern can be assumed to be ideal—plug flow—thereby simplifying the hydrodynamic modelling. Fixed beds do have limitations. In cases where catalyst deactivates with time, for example, in the case of coking of active sites or pore blocking, the coke is likely to progress down the bed resulting in a heterogeneous activity profile (Kaarsholm et al., 2007). For highly exothermic reactions temperature gradients and/or hot spots are problematic and the exact reaction temperature can be difficult to measure precisely. For intrinsic measurements, the catalyst particles should be small to avoid transport gradients but this leads to a high-pressure drop over the bed. Fluidized bed reactors have the advantage of isothermal operation due to rapid heat transfer by solids mixing. Uniform radial and axial temperature and the ability to easily measure temperature are additional advantages over fixed beds. The solids back-mixing not only ensures temperature uniformity but also a homogeneous radial and axial activity profile: deactivated catalyst is distributed equally throughout the reactor. The greatest drawback of the fluidized bed is the hydrodynamics, which is more complex compared to fixed bed due to the presence of bubbles. The effect of bubbles has been investigated for several decades and a large number of mathematical models have been proposed to characterise their hydrodynamics (Kunii and Levenspiel, 1991). At low gas velocities, single-phase axial dispersion models have shown good results (Lorences et al., 2006). Horio and Wen (1977) divided multi-phase models into three groups: level 1 includes two-phase models with several adjustable parameters that are not directly related to the bubble size: The Van Deemter model (1961) and the model of May (1959) are examples. Level 2 models relate the bed parameters to the bubble size that is treated as a constant or a fitted parameter. The model of Kunii and Levenspiel (1968) is included in this group where the bubble diameter is measured by intrusive probes. The third level includes the bubble diameter as a function of height and may also account for grid region and freeboard effects. Recent models of this group were proposed by Werther and Hartge (2004); Christensen et al. (2008); and Radmanesh et al. (2006). Grace (1982) showed that two-phase systems with plug flow in the bubble phase and either plug flow or a back mixed emulsion phase with mass transfer between the phases can predict fluidized bed reactor performance.

The mass transfer between the bubble and emulsion phases is a key parameter with regard to both overall reactor effectiveness and for reactor scale-up. The interphase mass transfer coefficient between the bubble and the emulsion phase is either calculated based on a correlation of Sit and Grace (1981) or it can be calcu-

lated separately including the interaction of the bubble and wake and emulsion (Kunii and Levenspiel, 1991).

Shaikh and Batran (2007) have further expanded the mass transfer term by including film resistance on the bubble side alongside the mass transfer coefficient between the emulsion and bubble phase. They conclude that this term is important for fast reactions.

In this article, the methanol to DME reaction in a gas–solid bubbling bed is reported over a range of gas velocities and bed heights. The catalyst was specifically designed for fluidized bed operation. Low gas velocities were used to approach ideal gas flow conditions while at the same time maintaining isothermal conditions. Kinetic expressions were derived from the experimental data employing a detailed two-phase fluidized bed model and an *n*-CSTR's in series model. The goal of this study is to establish the feasibility of using fluidized bed reactors to perform kinetic studies of fast and highly exothermic reactions.

## EXPERIMENTAL

### Equipment

The experiments were carried out in a 46 mm inner diameter quartz fluidized bed (Figure 1) with a 66 mm inner diameter disengagement zone. The total reactor height was 915 mm.

The gas entered the reactor at the bottom and uniform radial distribution was achieved through a high-pressure drop quartz frit.

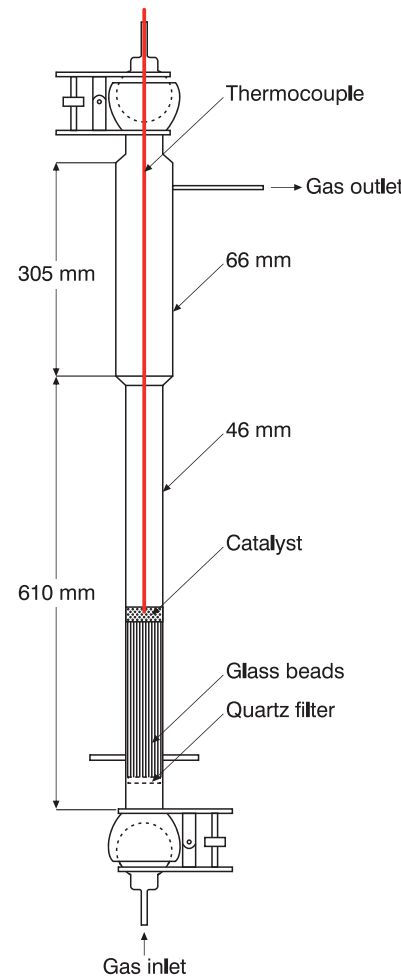


Figure 1. Drawing of the glass fluidized bed with glass beads, catalyst, and thermocouple.

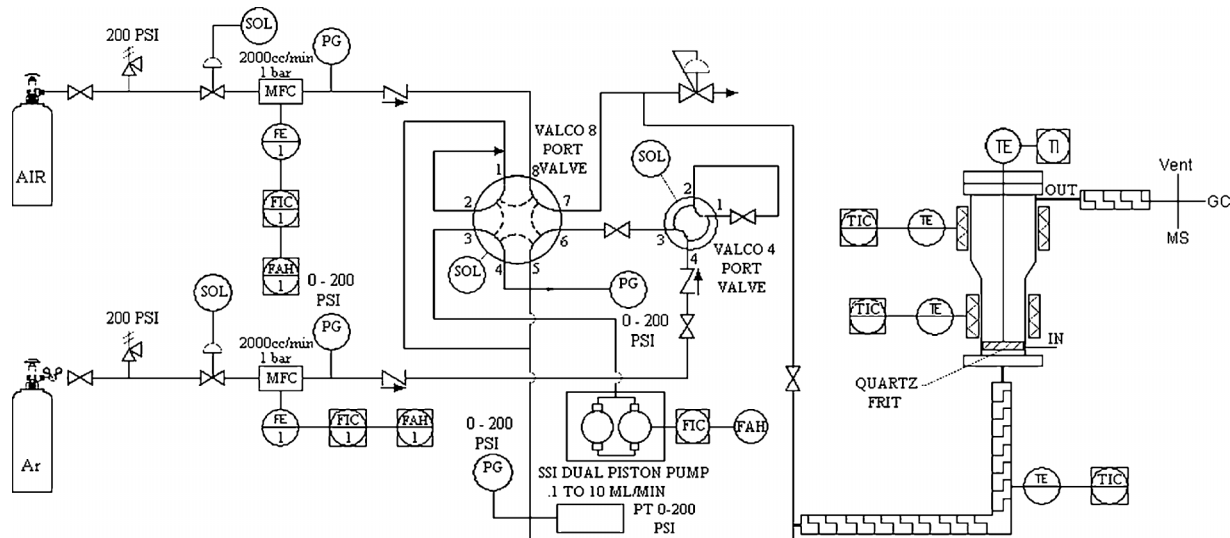


Figure 2. Schematic diagram of the experimental setup.

The reactor temperature was controlled by two electrical band heaters, one located in the fluidized bed zone and the other in the disengagement zone. A thermocouple inserted in the middle of the catalyst bed monitored the reaction temperature. Liquid methanol was fed from a dual piston pump and the gas was metered by Brooks mass flow controllers (MFC). The inlet stream was pre-heated to 150°C to ensure liquid feed was entirely vaporised. The effluent gas was analysed by a Hiden mass spectrometer QIC-20 (MS) and a Varian CP3800 GC. A diagram of the system is illustrated in Figure 2.

### Catalyst

The catalyst was composed of 10% CBV28014 (Zeolyst) imbedded in a Si/Al matrix consisting of Catapal B, Levasil 100 s/30%, and kaolin that was spray dried then calcined in air at 550°C for 4 h. The powder was contacted with a  $(\text{NH}_4)_2\text{HPO}_4$  solution and then dried and calcined so that the resulting catalyst contained 1.5% phosphorous.

The particle size distribution was measured on a Horiba LA-950 and the mean particle diameter was measured to be 108  $\mu\text{m}$ . The minimum fluidization velocity at ambient temperature and pressure was 0.0051 m/s in a 76 mm perspex column in which the tapped particle density and density at minimum fluidization were also measured. The catalyst properties are listed in Table 1.

### Experimental Conditions

For experiments conducted with  $<100\text{ g}$  of catalyst, glass beads with a particle diameter of 500  $\mu\text{m}$  were pre-charged to the ves-

sel in order to elevate the bed into the heating zone and thus ensure isothermal conditions. Cold flow experiments indicated that as long as the gas velocity was kept below the minimum fluidization velocity ( $u_{mf,gb}$ ) of the glass beads, mixing between the beads and the catalyst was negligible and most of the catalyst remained on top. When the gas velocity was increased above  $u_{mf,gb}$ , the beads and catalyst would form a homogeneous mixture. Most of the catalyst particles from the homogeneous mixture would return to the top of the bed when the gas velocity was subsequently reduced below  $u_{mf,gb}$ . However, a small fraction of the catalyst remained with the beads after reducing the gas velocity. In all experiments, the superficial gas velocity was maintained below  $u_{mf,gb}$ , thereby ensuring the catalyst remained above the beads.

The feed gas consisted of 5, 15, 30, and 33 mol% methanol in argon. The superficial gas velocity ranged from 0.45 to 8.4 cm/s and the experiments were conducted with four different catalyst loadings 25, 50, 100, and 200 g. Steady state was considered to be achieved when the product distribution was stable over a period of a few minutes on the MS.

The MS was calibrated with several mixtures of water, DME, methanol, and argon in the same range as the expected product distribution. The exit composition was also measured on a GC to verify the MS analysis. The retention times of the components were validated from binary gas mixtures of argon and the gas of interest except in the case of methanol which was done from a methanol-air mixture.

Four experiments were conducted to assess the residence time distribution (RTD). The first was with an empty vessel. The second was with 540 g of glass beads. In the third, 50 g of catalyst was placed on top of the glass beads. In the fourth experiment, the glass beads were removed and the reactor was charged with 220 g of catalyst. The experiments were carried out with argon as the tracer gas that would displace the air in the reactor as a result of switching the position of the 8-port Valco valve. To maintain steady conditions when switching the valve between air and argon, the tracer gas was vented to atmosphere at approximately the same pressure and flow rate as the air that was fed to the reactor. Therefore, when the multiport valve was switched, the transient response of the MFC to reach a steady flow rate was avoided. Switching in this manner is characterised as a Heavy-

Table 1. Particle properties of the catalyst

$d_p < 45$	0.4	$200 < d_p > 229$	2.9
$45 < d_p < 68$	4.7	$229 < d_p < 262$	1.6
$68 < d_p < 89$	16.6	$262 < d_p < 350$	1.3
$89 < d_p < 102$	15.5	$d_p$	108 $\mu\text{m}$
$102 < d_p < 117$	16.7	$u_{mf}$	0.0051 m/s
$117 < d_p < 133$	15.3	$\rho_p$	1270 kg/m <sup>3</sup>
$133 < d_p < 153$	11.9	$\rho_{tapped}$	855 kg/m <sup>3</sup>
$153 < d_p < 175$	8.1	$\rho_{mf}$	744 kg/m <sup>3</sup>
$175 < d_p < 200$	5.0	$\varepsilon_{mf}$	0.405

**Table 2.** *n*-CSTR model parameters for the RTD experiments done at  $u_0$  0.052 m/s

Catalyst amount	$\sigma^2$ (s)	$t_m$ (s)	<i>N</i>	<i>Pe</i>
540 g glass beads	573	26.8	28	54
540 g glass beads + 50 g catalyst	428	26.7	27	52
220 g catalyst	618	28.0	15	28

side unit step function whose first derivative is the Dirac delta pulse. The change in exit gas compositions was recorded at the exit of the reactor by MS at a frequency of 4.4 Hz.

## EXPERIMENTAL RESULTS

### RTD

The E-curve for three experiments conducted at 5.4 cm/s are shown in Figure 3. Figure 3A corresponds to experiments made with 540 g of glass beads. In Figure 3B, 50 g of catalyst were loaded to the top of the glass beads and in Figure 3C, the glass beads were withdrawn and 220 g of catalyst was charged to the vessel. The curves in Figure 3A,B are almost identical suggesting that 50 g of catalyst has inconsequential effect on the gas flow pattern. However, with 220 g of catalyst, the shape of the curve, as shown in Figure 3C, is altered significantly. The mean residence time is higher for the last experiment because the volume of catalyst is less than half the volume of glass beads. The peak shape is much broader, even though there are fewer solids, indicating that the flow pattern is less ideal.

The RTD of the empty vessel—including wind box, bed, free-board, and disengagement zone was similar to the RTD measured with glass beads. As shown in Table 2, the variance was highest for the experiments with 220 g of catalyst, which corresponds to 15 *n*-CSTRs in series. The variance is lower with the glass beads and the flow is more ideal and can be approximated by almost 30 *n*-CSTRs in series. The variance includes all piping plus windbox and disengagement section. To approximate the hydrodynamics of the 220 g of catalyst, we subtract the variance of the experiment with the gas beads (and account for the difference in the volume of solids) resulting in 6 *n*-CSTRs in series. The *Pe* number is related to the number of CSTRs series by the relation  $Pe = 2(n - 1)$  and equals 10 and the axial dispersion is  $0.0008 \text{ m}^2/\text{s}$ , which corresponds to the values reported by Lorences et al. (2006). They showed that as the gas velocity approached  $u_{mf}$  the flow pattern became closer to ideal. Our experiments indicated that at a gas velocity 10 times  $u_{mf}$ , gas approached plug flow as the solids inventory was reduced.

### Methanol to DME

The experimental results from the MeOH/DME reaction with 25, 50, 100, and 200 g of catalyst are given in Table 3 including temperature, equilibrium constant, flows, catalyst inventory, and exit concentrations. During experiments 20–46, there was a problem with the thermocouple monitoring the fluidized bed temperature resulting in an offset in the actual value. Temperature measurements at different points in the bed during reaction did not indicate a problem with uniformity in the bed and only small differences of 1–2°C were observed. The maximum uncertainty is estimated to be  $\pm 2\%$  on the conversion to equilibrium.

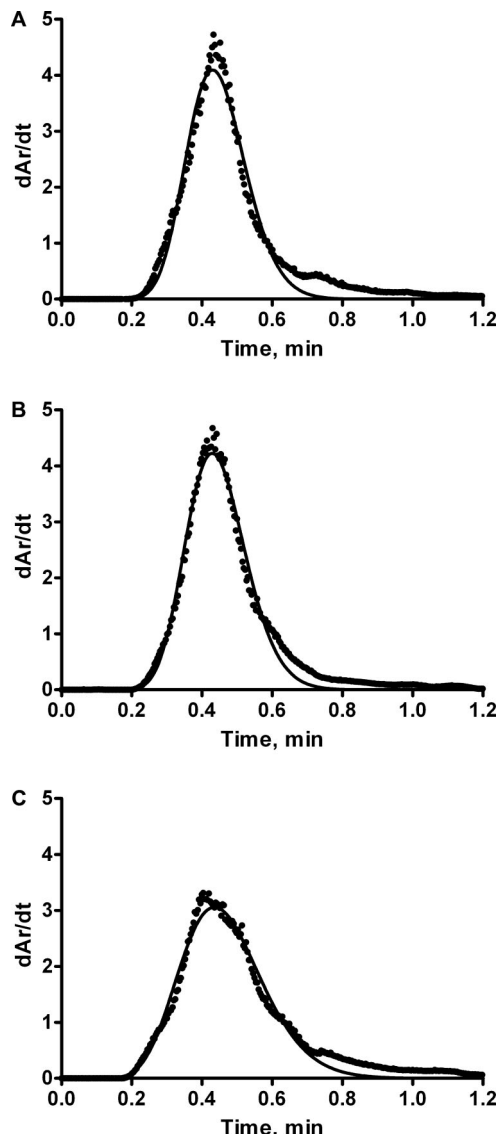


**Figure 3.** RTD experimental results over the fluidized bed with a gas velocity of 5.4 cm/s. A: reactor loaded with 540 g glass beads. B: Reactor loaded with 540 g glass beads and 50 g of catalyst. C: Reactor loaded with 220 g of catalyst. Experimental data represented by dots and *n*-CSTR model with a line.

The MS was set to monitor not only Ar, MeOH, DME, and H<sub>2</sub>O but also other hydrocarbon fractions. At 325°C, alkene production became significant, thus most of the data at this temperature were disregarded in the kinetic modelling. MS traces of experiments 20–24 are shown in Figure 4. The fluidized bed was operating at gas velocities close to  $u_{mf}$  at 30 min and the DME and H<sub>2</sub>O concentrations were high while the methanol concentration was close to equilibrium. At 35 min, the gas velocity was increased to 0.89 cm/s and the DME and the water concentrations dropped while the methanol increased. The same trend is observed for each of the subsequent feed rate increases. The new product distribution was established within 2–5 min depending on flow rate and the change is clearly defined. A low level of methane was recorded in all experiments.

The conversion to equilibrium based on a gas sample measured by GC was 96.4% in experiment 31 and 88.9% in experiment 39 which was in agreement with the MS analysis. From the GC data

**Table 3.** Experimental data obtained—all flows are listed at STP conditions

Exp. no.	Temp. (°C)	Cat. (g)	Q <sub>MeOH</sub> (mL/min)	Q <sub>Ar</sub> (mL/min)	u <sub>0</sub> cm/s	K <sub>eq</sub>	γ <sub>MeOH</sub>	γ <sub>DME</sub>	Conv. to EQ (% ± 2%)	Total conv. (%)
1	250	50	16.8	334	0.67	16.0	0.007	0.020	95.8	85.2
2	250	50	50.5	947	1.92	16.0	0.010	0.021	91.2	81.1
3	250	50	124	2340	4.73	16.0	0.012	0.019	86.3	76.7
4	250	200	50.5	947	1.92	16.0	0.007	0.022	96.1	85.5
5	250	200	124	2334	4.73	16.0	0.008	0.021	93.9	83.5
6	275	50	50.5	947	2.01	12.8	0.009	0.021	94.1	82.6
7	275	50	124	2340	4.95	12.8	0.010	0.020	90.4	79.3
8	250	50	39.3	214	0.49	16.0	0.026	0.064	93.4	83.0
9	250	50	152	858	1.94	16.0	0.050	0.050	74.6	66.4
10	250	50	382	2160	4.88	16.0	0.075	0.038	56.2	50.0
11	275	50	39.3	214	0.51	12.8	0.026	0.065	94.9	83.3
12	275	50	152	858	2.03	12.8	0.034	0.058	87.8	77.1
13	275	50	382	2160	5.12	12.8	0.044	0.053	80.4	70.5
14	250	50	157	355	0.98	16.0	0.089	0.109	79.8	70.9
15	250	50	309	710	1.96	16.0	0.150	0.076	56.6	50.4
16	250	50	792	1840	5.05	16.0	0.209	0.046	34.3	30.5
17	275	50	157	355	1.03	12.8	0.066	0.120	89.4	78.4
18	275	50	309	710	2.05	12.8	0.081	0.111	83.5	73.2
19	275	50	792	1840	5.29	12.8	0.121	0.090	68.2	59.8
20	278	25	78.5	154	0.47	12.5	0.060	0.139	93.9	82.3
21	277	25	157	307	0.94	12.6	0.090	0.125	83.9	73.5
22	278	25	309	613	1.86	12.5	0.122	0.107	72.7	63.7
23	279	25	791	1580	4.82	12.4	0.183	0.075	51.5	45.2
24	277	25	1250	2560	7.79	12.6	0.224	0.053	36.6	31.9
25	280	50	78.5	154	0.47	12.3	0.059	0.140	94.2	82.6
26	277	50	157	307	0.94	12.6	0.075	0.132	88.9	78.0
27	278	50	309	613	1.86	12.5	0.088	0.123	84.1	73.6
28	279	50	791	1580	4.82	12.4	0.138	0.098	67.0	58.7
29	278	50	1250	2560	7.71	12.5	0.174	0.077	53.6	47.0
30	278	100	78.5	154	0.47	12.5	0.046	0.146	98.7	86.3
31	279	100	157	307	0.94	12.4	0.053	0.143	96.4	84.3
32	279	100	309	613	1.87	12.4	0.064	0.135	92.3	80.8
33	282	100	791	1580	4.84	12.1	0.093	0.120	82.5	72.2
34	284	100	1250	2560	7.79	11.9	0.115	0.107	74.5	65.0
35	287	200	78.5	154	0.48	11.6	0.044	0.147	99.8	87.0
36	288	200	157	307	0.96	11.5	0.046	0.146	99.1	86.4
37	288	200	309	613	1.90	11.5	0.049	0.143	98.0	85.3
38	289	200	791	1580	4.90	11.4	0.062	0.136	93.5	81.5
39	290	200	1250	2560	7.88	11.3	0.073	0.128	88.9	77.7
40	325	25	78.5	154	0.51	8.66	0.044	0.147	101.8	87.0
41	325	25	157	307	1.01	8.66	0.044	0.148	101.8	87.1
42	325	25	309	613	2.02	8.66	0.054	0.140	98.1	83.8
43	325	25	791	1580	5.22	8.66	0.073	0.130	91.3	78.0
44	325	25	1250	2560	8.37	8.66	0.087	0.121	86.0	73.6
45	325	50	791	1580	5.22	8.66	0.061	0.136	95.6	81.8
46	325	50	1250	2560	8.37	8.66	0.069	0.130	92.5	79.1

the level of methane was found to be 0.25% on carbon basis, which is considered negligible.

Due to a slightly declining background level of water in the MS trace, the water fraction was calculated based on the DME, which had a much greater sensitivity. A graphical representation of the methanol conversion of experiments 20–39 is shown in Figure 5. At low gas velocities close to  $u_{mf}$ , methanol conversion approached 100%. With 200 g of catalyst, the methanol conversion reached equilibrium at the three lowest gas velocities. The consistency of the data was confirmed by comparing methanol conversion at two conditions with the same contact time. For example, methanol conversion is about 70% at a gas velocity of 0.47 cm/s with 25 g of catalyst and at 1.86 cm/s and 100 g of catalyst.

## MODELLING

### Kinetics

Mollavali et al. (2008) recently studied the methanol to DME reaction (Equation 1) and summarised the published kinetic models with reaction orders of  $\frac{1}{2}$ , 1, and 2.



Calculations of the reaction order by the half-lives method from the fluidized bed data gives a reaction order in the range 1.75–2 and therefore a second-order reaction has been assumed in this work.

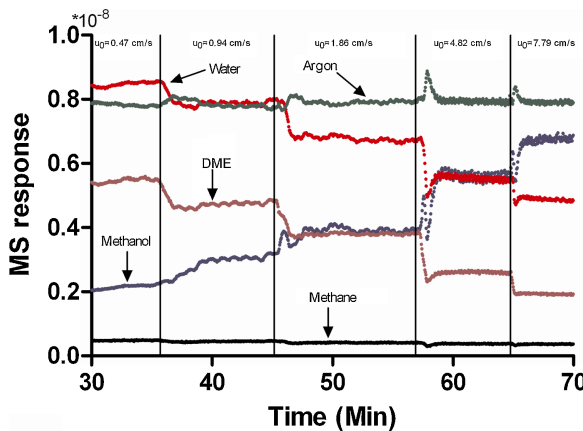


Figure 4. MS results from experiments done at 275°C with 25 g of catalyst.

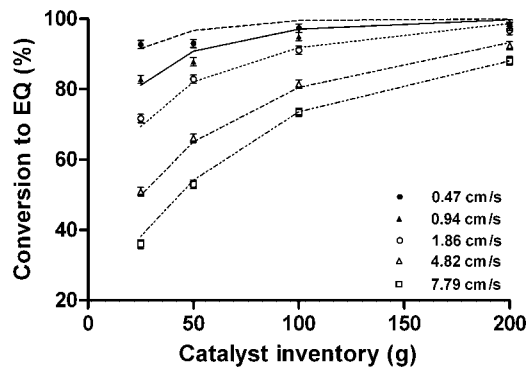


Figure 5. Conversion of methanol to DME and water based on equilibrium conversion as function of catalyst amount at five different gas velocities (experiments 20–39). Lines are the model predictions using kinetic model Equation (5) and 6 CSTR's in series.

Due to the high conversion levels the reverse reaction also has to be included in the kinetic expression. Literature models that include the equilibrium term are given in Table 4. The absorption term of DME is neglected in all of the models because it is much smaller than the absorption of methanol and water (Berčić and Levec, 1992).

A simple model for the methanol to DME reaction is proposed where methanol is absorbed on a active catalyst site (Equation 2), two absorbed methanol species then react to form DME and an absorbed water molecule (Equation 3). This reaction is considered to be the rate-determining step. Finally, the water is desorbed (Equation 4).



Table 4. Kinetic models including the reverse term

Model	Equation	Refs.
1	$-r_{\text{MeOH}} = \frac{k(C_M - C_W C_D / (K_{\text{eq}} C_M))}{(1 + K_M C_M + C_W / K_W)}$	Mollavali et al. (2008)
2	$-r_{\text{MeOH}} = \frac{k(C_M^2 / C_W - C_D / K_{\text{eq}})}{(1 + K_M C_M + K_W C_W)^2}$	Lu et al. (2004)
3	$-r_{\text{MeOH}} = \frac{k K_M^2 (C_M^2 - C_W C_E / K_{\text{eq}})}{(1 + 2(K_M C_M)^{0.5} + K_W C_W)^4}$	Berčić and Levec (1992)



An expression for the methanol reaction rate may be derived from Equations (2)–(4) and is given by Equation (5). This kinetic expression is compared to the model of Berčić and Levec (1992) with adjusted parameters to account for the temperature interval and catalyst composition.

$$-r_{\text{MeOH}} = \frac{k C_M^2 \left( 1 - \frac{C_D C_W}{C_M^2 K_{\text{eq}}} \right)}{(1 + K_M C_M + K_W C_W)^2} \quad (5)$$

Grace (1982) divides first-order kinetics into three categories slow, intermediate, and fast reactions in fluidized beds based on their reaction rate constant. Slow reactions are controlled by reaction kinetics while intermediate reactions can be controlled by either reaction rates or mass transfer between the bubble and emulsion phases. Fast reactions are characterised by  $k$  values above  $5 \text{ s}^{-1}$  and slow reactions have  $k$  values below  $0.5 \text{ s}^{-1}$ . For a first-order reaction  $t_{1/2} = \ln(2)/k$  and a fast reaction in this view is a reaction with a half-life below 0.14 s and a slow reaction with a half-life above 1.4 s. Using the same criteria for second-order reactions, we categorise the methanol dehydration reaction as either fast, intermediate, or slow. The average half-life from the experiments can be calculated by Equation (6) ignoring the reverse reaction:

$$t_{1/2} = \frac{\tau}{\frac{1}{1-X} - 1} \quad (6)$$

where  $X$  is the total conversion of methanol and  $t$  is the residence time in the bed. For experiments 43, 44, and 46, the average half-life is 0.08–0.13 s which is below the criteria for a fast reaction and it would be assumed that the mass transport between the emulsion and bubble will play a role in the modelling of this data. For all the experiments below 300°C, the average half-life is above 0.5 s and the reactions rates are considered to be in the intermediate region. The experimental data with conversion to equilibrium above 95% all have an average half-life above 1.4 s and slow reaction rates which would also be expected for second-order reactions close to equilibrium where the reaction rate is reduced.

### Fluidized Bed Model

The fluidized bed has been characterised with a two zone fluidized bed model as well as an  $n$ -CSTR's in series model with six CSTRs in series. The number of CSTR's in series has been considered to be constant over the range of gas velocities and catalyst inventory. Improving the  $n$ -CSTR's in series model with the numbers of CSTR's as function of gas velocity and catalyst inventory is possible but has not been included in this study. The two-phase model is well described in the literature and has recently been used by Werther and Hartge (2004) to model industrial fluidized bed reactors and by Abba et al. (2003) where it was used as part of a comprehensive model to characterise fluidization from bubbling conditions to fast fluidization. The differences in the two models are due to different assumptions regarding the hydrodynamics. In this work the following assumptions are made:

- Gas flows in the axial direction only—dispersion in the radial direction is neglected (with the exception of interphase mass transfer).
- Interphase mass transfer between bubble and emulsion phase.
- No catalyst in the bubble phase.
- The activity of the catalyst is considered constant.

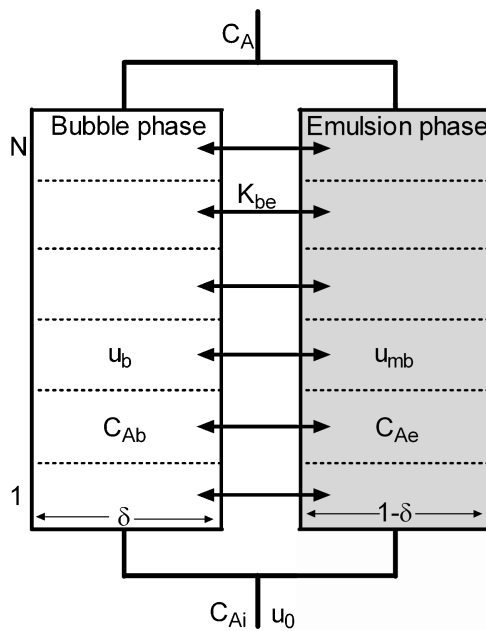


**Figure 6.** Schematic of the two-phase fluidized bed model

The mass balance of the bubble and emulsion phases of the model can be written as:

$$\text{Bubble phase: } -u_b \frac{dC_{i,b}}{dz} = K_{be}(C_{i,b} - C_{i,e}) \quad (7)$$

$$\text{Emulsion phase: } u_{\text{mb}} \frac{dC_{i,e}}{dz} = \frac{\delta}{(1-\delta)} K_{\text{be}} (C_{i,b} - C_{i,e}) + (1 - \varepsilon_{\text{mf}}) \rho_p (-r_i) \quad (8)$$

The model has been implemented in Fortran as two parallel CSTRs in series with mass transfer between the two. The implemented equations are given in Equations (9) and (10) and a schematic diagram is shown in Figure 6.

The CSTR volume is based on equal catalyst amount, for example, constant emulsion volume, which makes the CSTR's volume in the bubble phase dependent on the bubble velocity:

$$F_b x_{b,i,n} = F_b x_{b,i,n-1} - \frac{\delta}{1-\delta} V_e K_{be} (\rho_g x_{b,i,n} - \rho_g x_{e,i,n}) \quad (9)$$

$$F_{\text{e}}x_{\text{e},i,n} = F_{\text{e}}x_{\text{e},i,n-1} + \frac{\delta}{1-\delta} V_{\text{e}} K_{\text{be}} (\rho_{\text{g}}x_{\text{b},i,n} - \rho_{\text{g}}x_{\text{e},i,n}) + W(-r_i) \quad (10)$$

The kinetic rate parameters were fit to the experimental data using the Simplex method in which the object function given by Equation (11) was minimised:

$$\Phi = 1 - \frac{\sum_n (x_{i,n,\text{cal}} - x_{i,n,\text{exp}})^2}{\sum_n (x_{i,n,\text{exp}} - \bar{x}_{i,\text{exp}})^2} = 1 - R^2 \quad (11)$$

The hydrodynamic correlations used in this work are given in Table 5. The bubble diameter was calculated based on the correlation of Mori and Wen (1975) and the mass transfer coefficient is based on Sit and Grace's (1981) work. Since the catalyst belongs to the Geldart group A powder, the void fraction in the emulsion phase is assumed to be equal to that measured at the minimum bubbling velocity.

## MODELLING RESULT AND DISCUSSION

All parameters in the fluidized bed model, besides the molecular diffusion coefficient, are derived from the experimental data or the hydrodynamic correlations. The molecular diffusion coefficient varies between 0.2 and 0.6 cm<sup>2</sup>/s for the binary mixtures and for the modelling of the fluidized bed an average value of 0.4 cm<sup>2</sup>/s has been used. The model calculations were reasonably independent of assumed value of the molecular diffusion. The models parameters were fit to the data in experiments 1–19. The parameters and goodness of fit (characterised by the regression coefficient  $R^2$ ) to the experimental data for the fluidized bed model and six CSTR's in series are given in Table 6.

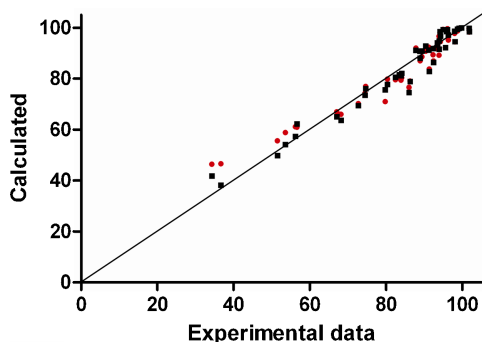
Activation energies of the heat of adsorption terms were neglected in the fitting since the data were insufficient to reliably characterise this parameter. Rather, we have adopted the values proposed by Berčić and Levec (1992). The lack of temperature dependency in the absorption term for the proposed model might explain some of the difference in the activation energy seen between the two models since the absorption can influence the reaction rate. The kinetic model of Equation (5) shows the best result when coupled with six CSTR's in series compared to the other kinetic and reactor model. Modelling the rest of the data set (experiments 20–46) shows a very good fit to the data derived from the first 19 experiments. In Figure 5 the data from experiments 20 to 39 is plotted together with the model prediction. The overall agreement is very good and only at high conversion does

**Table 5.** Hydrodynamic correlations—the correlation for bubble diameter is in cm and not in meters

Variable	Correlation	Refs.
Mass transfer coefficient	$k_{be} = \frac{u_{mb}}{3} + \left( \frac{4D_{e,mf}\bar{u}_b}{\pi d_b} \right)^{1/2}$	Sit and Grace (1981)
Bubble diameter	$d_b = d_{bm} - (d_{bm} - d_{b0})\exp\left(\frac{-0.3z}{D_t}\right)$ $d_{b0} = 0.00376(u_0 - u_{mb})^2, d_{bm} = 0.652(A_t(u_0 - u_{mb}))^{0.4}$	Mori and Wen (1975)
Bubble velocity	$u_b = u_0 - u_{mb} + 0.711(gd_b)^{1/2}$	
Minimum fluidization velocity	$u_{mf} = \frac{\mu}{d_p \rho_g} \left[ \left[ (33.7)^2 + 0.0408 \left( \frac{d_p^3 \rho_g (\rho_p - \rho_g) g}{\mu^2} \right) \right]^{1/2} - 33.7 \right]$	Wen and Yu (1966)
Minimum bubbling	$\frac{u_{mb}}{u_{mf}} = \frac{2300 \rho_g^{0.126} \mu^{0.523} \exp(0.716F)}{d_p g^{0.934} (\rho_p - \rho_g)^{0.934}}$	Abrahamsen and Geldart (1980)
Bubble fraction	$\delta = \frac{u_0 - u_{mb}}{u_b - u_{mb}}$	

**Table 6.** Best fit parameters for the two kinetic and reactor models and the level of fit to the experimental data

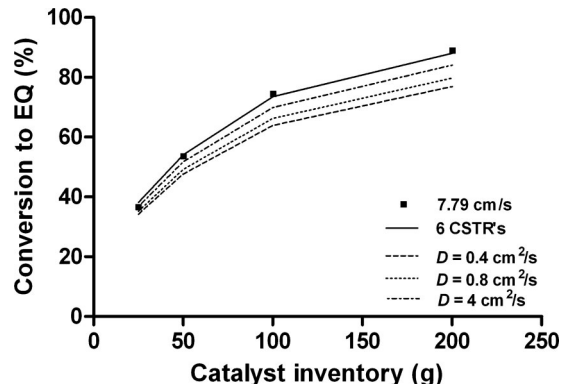
Kinetic model	Reactor model	$k$ (m <sup>6</sup> /(kg s kmol))	$E_a$ (kcal/mol)	$K_W$ (m <sup>3</sup> /kmol)	$K_m$ (m <sup>3</sup> /kmol)	$R^2$ (exps. 1–19)	$R^2$ (all expts.)
Equation (5)	Fluidized bed	21 900	24.5	47 000	14 000	0.918	0.901
	6 CSTR's	21 400	22.1	47 000	15 000	0.934	0.940
Berčić and Levec (1992)	Fluidized bed	0.619	33.0	590	48	0.906	0.884
	6 CSTR's	0.677	32.2	480	30	0.910	0.925

**Figure 7.** Model predictions versus experimental with six CSTR's in series. (■) Model Equation (5) and (●) model of Berčić and Levec (1992).

the model over predict the actual conversion. The ability of the CSTR's in series model to characterise the experimental data better than the fluidized bed model indicates that the mass transfer between the bubble and emulsion phase is not a limiting factor. This observation is confirmed based on the fact that very high levels of conversion were achieved, which would have been difficult if mass transfer between the emulsion and bubble was limiting the reaction rate.

A parity plot of all the data compared to the model estimations with the use of the kinetic model Equation (5) and the model of Berčić and Levec (1992) are given in Figure 7. Both models characterise the experimental data at high conversion but at low conversion, the model predictions given by Equation (5) are superior. The absorption term—which is the major difference between the two models—has a large influence on the reaction rate. Overall the predicted conversions are within 5% of the measured values.

The influence of the mass transfer coefficient in the two-phase model has been investigated by using the best fit kinetic parameters derived from the CSTR's in series model. In Figure 8, the effect of changing the mass transfer coefficient on conversion at various levels of catalyst inventory is represented. At low catalyst inventory, there is little effect of diffusivity on the predicted conversion. The effect increases with the catalyst inventory, which is due to the increase in bubble size. The deviation is most significant at

**Figure 8.** Effect of the molar diffusion coefficient ( $D$ ) with the use of the best fit parameters for 6-CSTR's in series with the two-phase model and the kinetic model of Equation (5). The experimental data were collected at 275°C and a superficial gas velocity of 7.79 cm/s.

200 g but even changing the diffusion coefficient by an order of magnitude only changes the calculated conversion by about 5%.

The conversion measured in the present work is often close to equilibrium, which is not ideal for a kinetic study. The operational range in fluidized beds may be limited by gas velocity and catalyst inventory. Deviation from plug flow increases with gas velocity thereby rendering the interpretation of experimental data more difficult. Decreasing the catalyst inventory further leads to a very shallow bed and the possibility of gas by-passing must be considered. Changing the temperature is the best option to investigate a large range of conversion and lowering the temperature below 250°C would be desirable to validate the kinetic model at low conversions.

Data from a 4 mm quartz fixed bed reactor together with predictions of the conversion using Equation (5) are given in Table 7. The predicted conversion is lower than the measured value and the difference increases with temperature. The large difference between model predictions and experimental data is most likely due to temperature gradients in the bed caused by the exothermic reaction, which increases with increased reaction temperature and thus higher reaction rate.

**Table 7.** Fixed bed experiments in a 4 mm inner diameter quartz reactor

Temp. °C	Cat. (g)	$Q_{\text{MeOH}}$ (mL/min)	$Q_{\text{Ar}}$ (mL/min)	$u_0$ (cm/s)	$K_{\text{eq}}$	$\gamma_{\text{MeOH}}$	$\gamma_{\text{DME}}$	Conv. to EQ (% ± 2%)	Model prediction
250	0.1	1.3	12	3.39	16.0	0.066	0.017	39	50.2
250	0.1	2.8	25	7.05	16.0	0.070	0.015	34	34.1
275	0.1	1.3	12	3.55	12.8	0.027	0.036	83	74.6
275	0.1	2.8	25	7.39	12.8	0.034	0.033	75	58.7
275	0.1	5.6	50	14.8	12.8	0.057	0.022	50	42.8
300	0.1	1.3	12	3.71	10.4	0.016	0.042	97	91.5
300	0.1	2.8	25	7.73	10.4	0.019	0.040	93	80.2
300	0.1	5.6	50	15.5	10.4	0.026	0.037	85	66.0
300	0.1	1.3	12	3.71	10.4	0.014	0.043	99.4	91.5

Fluidized bed reactors have clear advantages over fixed bed reactors for measuring reaction kinetics of fast and highly exothermic (or endothermic) reactions. In this work, we demonstrate that by operating at gas velocities close to  $u_{mf}$ , the gas flow pattern approaches plug flow. At velocities as much as 10 times  $u_{mf}$ , the gas phase can be modelled assuming as many as six CSTRs in series. Maintaining isothermal conditions both radially and axially is critically important for modelling. Furthermore, an accurate measure of the temperature is important and both of these phenomena are more problematic in fixed bed reactors: small uncertainties in temperature result in a poor estimation of the reaction rate and activation energy. Measuring the temperature precisely, avoiding hot spots and minimising gradients are critically important. This is difficult in fixed bed reactors (Fogler, 2005) and thus one is forced to dilute the catalyst with inert and operate with low feed concentrations. Diluting the catalyst introduces the possibility of bypassing and it has been shown to influence the observed conversion especially at conversions above 0.4 (Berger et al., 2002).

## CONCLUSION

The dehydration kinetics of methanol to DME was measured in a fluidized bed at gas velocities from  $u_{mf}$  to almost 20 times  $u_{mf}$ . Kinetic expressions were derived from the experimental data based on both a detailed two phase fluidized hydrodynamic model and a one-dimensional  $n$ -CSTR in series model. The kinetics based on the  $n$ -CSTR hydrodynamics fit the experimental data extremely well and was superior to the two-phase fluidized bed model. This was observed for both the proposed kinetic model and the literature model of Berčić and Levec (1992). The fluidized bed was shown to be a good reactor type for the kinetic modelling of the methanol to DME reaction due to the isothermal conditions and the conversions that could be obtained at relatively low gas velocities. Other exothermic reactions where hotspots or temperature gradients are of concern should consider fluidized bed reactors as a viable alternative to generate kinetic data. Due to restraints on the catalyst inventory and gas velocities the conversion range at a given temperature will be dependent on the catalytic system.

## NOMENCLATURE

$A_t$	cross-sectional area of the fluidized bed (m <sup>2</sup> )
$C$	molar concentration (kmol/m <sup>3</sup> )
$D$	molar diffusion coefficient (m <sup>2</sup> /s)
$D_t$	reactor diameter (m)
$d_p$	mean particle diameter (m)
$d_b$	bubble diameter (m)
$d_{b0}$	initial bubble diameter at the distributor (m)
$d_{bm}$	maximum bubble diameter (m)
$E_a$	activation energy (kJ/mol)
$F$	fine fraction
$F_b$	flow rate in bubble phase (kmol/s)
$F_e$	flow rate in emulsion phase (kmol/s)
$g$	gravity (m/s <sup>2</sup> )
$K_{eq}$	equilibrium constant
$k$	reaction rate constant (m <sup>6</sup> /kmol s)
$K_{be}$	bubble to emulsion mass transfer coefficient (s <sup>-1</sup> )
$k_{be}$	bubble to emulsion mass transfer coefficient (m/s)
$N$	number of CSTR's
$Pe$	Peclet number ( $Pe = U_g L/D$ )
$r_i$	reaction rate of component $i$ (kmol/kg s)
$t_{1/2}$	halftime (s)

$t_m$	mean residence time (s)
$u_{mf}$	minimum fluidization velocity (m/s)
$u_{mb}$	minimum bubbling velocity (m/s)
$u_{mb,gb}$	minimum bubbling velocity of glass beads (m/s)
$u_b$	bubble velocity (m/s)
$u_0$	superficial gas velocity (m/s)
$V_e$	volume of emulsion (m <sup>3</sup> )
$W$	catalyst weight (kg)
$Q$	gas flow (mL/min)
$X$	total conversion
$x$	mole fraction
$y$	mole fraction of gas
$z$	height in bed (m)

## Greek Symbols

$\delta$	bubble phase volumetric fraction
$\varepsilon_{mf}$	void fraction at minimum fluidization
$\mu$	gas viscosity (kg/m s)
$\sigma^2$	variance
$\rho_p$	particle density (kg/m <sup>3</sup> )
$\rho_{tapped}$	tapped density (kg/m <sup>3</sup> )
$\rho_{mf}$	minimum fluidization density (kg/m <sup>3</sup> )
$\rho_g$	gas density (kg/m <sup>3</sup> )
$\tau$	residence time (s)

## Subscripts

exp	experimental
calc	calculated
$n$	CSTR number
$i$	species
be	bubble to emulsion
b	bubble
e	emulsion

## REFERENCES

- Abba, I. A., J. R. Grace, H. T. Bi and M. L. Thompson, "Spanning the Flow Regimes: Generic Fluidized-Bed Reactor Model," *AIChE J.* **49**, 1838–1848 (2003).
- Abrahamsen, A. R. and D. Geldart, "Behaviour of Gas-Fluidized Beds of Fine Powders Part 1. Homogeneous Expansion," *Powder Technol.* **26**, 35–46 (1980).
- Berčić, G. and J. Levec, "Intrinsic and Global Reaction Rate of Methanol Dehydration Over  $\gamma$ -Al<sub>2</sub>O<sub>3</sub> Pellets," *Ind. Eng. Chem. Res.* **31**, 1035–1040 (1992).
- Berger, R. J., J. P. Ramírez, F. Kapteijn and J. A. Moulijn, "Catalyst Performance Testing: Bed Dilution Revisited," *Chem. Eng. Sci.* **57**, 4912–4932 (2002).
- Christensen, D., D. Vervloet, J. Nijenhuis, B. G. M. van Wachem, J. R. van Ommen and M.-O. Coppens, "Insights in Distributed Secondary Gas Injection in a Bubbling Fluidized Bed via Discrete Particle Simulations," *Powder Technol.* **183**, 454–466 (2008).
- Fogler, H. S., "Elements of Chemical Reaction Engineering," 4th ed., Prentice Hall, New Jersey (2005).
- Grace, J. R., in: G. Hetsroni, Ed., "Handbook of Multiphase Systems," Chapter 8: Fluidized-Bed Reactors. Hemisphere-McGraw Hill, New York (1982).
- Gray, C. and G. Webster, "A Study of Dimethyl Ether (DME) as an Alternative Fuel for Diesel Engine Applications," *Transport Canada Publication No.: TP 13788E*, May (2001).

- Horio, M. and C. Y. Wen, "An Assessment of Fluidized-Bed Modelling," *AIChE Symp. Ser.* **73**, 9–21 (1977).
- Kaarsholm, M., F. Joensen, J. Nerlov, R. Cenni, J. Chaouki and G. S. Patience, "Phosphorous Modified ZSM-5: Deactivation and Product Distribution for MTO," *Chem. Eng. Sci.* **62**, 5527–5532 (2007).
- Keil, F. J., "Methanol-to-Hydrocarbons: Process Technology," *Micropor. Mesopor. Mat.* **29**, 49–66 (1999).
- Kunii, D. and O. Levenspiel, "Bubbling Bed Model. Model for the Flow of Gas Through a Fluidized Bed," *I&EC Fundam.* **7**(3), 446–452 (1968).
- Kunii, D. and O. Levenspiel, "Fluidization Engineering," Butterworth-Heinemann series in chemical engineering, Newton, MA (1991).
- Lorences, M. J., J.-P. Laviolette, G. S. Patience, M. Alonso and F. V. Díez, "Fluid Bed Gas RTD: Effect of Fines and Internals," *Power Technol.* **168**, 1–9 (2006).
- Lu, W.-Z., L.-H. Teng and W. D. Xiao, "Simulation and Experiment Study of Dimethyl Ether Synthesis From Syngas in a Fluidized-Bed Reactor," *Chem. Eng. Sci.* **59**, 5455–5464 (2004).
- May, W. G., "Fluidized-Bed Reactor Studies," *Chem. Eng. Prog.* **55**(12), 49–56 (1959).
- Mollavali, M., F. Yaripour, H. Atashi and S. Sahebdelfar, "Intrinsic Kinetic Study of Dimethyl Ether Synthesis from Methanol on  $\gamma$ -Al<sub>2</sub>O<sub>3</sub> Catalysts," *Ind. Eng. Chem. Res.* **47**, 2365–3273 (2008).
- Mori, S. and Y. Wen, "Estimation of Bubble Diameter in Gaseous Fluidized Beds," *AIChE J.* **21**(1), 109–115 (1975).
- Radmanesh, R., J. Chaouki and C. Guy, "Biomass Gasification in a Bubbling Fluidized Bed Reactor: Experiments and Modeling," *AIChE J.* **52**(12), 4258–4272 (2006).
- Semelsberger, T. A., R. L. Borup and H. L. Greene, "Dimethyl Ether (DME) as an Alternative Fuel," *J. Power Sourc.* **156**, 497–511 (2006).
- Shaikh, A. A. and H. Batran, "On Bubble-Side Transport Limitations in Catalytic Fluid-Bed Reactors," *Chem. Eng. Res. Des.* **85**, 1215–1218 (2007).
- Sit, S. P. and J. R. Grace, "Effect of Bubble Interaction on Interphase Mass Transfer in Gas Fluidized Beds," *Chem. Eng. Sci.* **36**, 327–335 (1981).
- Van Deemter, J. J., "Mixing and Contacting in Gas-Fluidized Beds," *Chem. Eng. Sci.* **13**(3), 143–154 (1961).
- Wen, C. Y. and Y. H. Yu, "Mechanics of Fluidization," *Chem. Eng. Prog. Symp. Ser.* **62**, 100–111 (1966).
- Werther, J. and E.-U. Hartge, "Modeling of Industrial Fluidized-Bed Reactors," *Ind. Eng. Chem. Res.* **43**, 5593–5604 (2004).

---

*Manuscript received March 1, 2009; revised manuscript received March 9, 2010; accepted for publication March 12, 2010.*